

T H E U N I V E R S I T Y O F M I C H I G A N

COLLEGE OF ENGINEERING
Department of Electrical Engineering
Space Physics Research Laboratory

Technical Report

ON THE OPTIMIZATION OF THE
SPACE PHYSICS RESEARCH LABORATORY ULTRAHIGH VACUUM SYSTEM

Adel Eltimsahy

ORA Project 08902

under contract with:

NATIONAL AERONAUTICS AND SPACE ADMINISTRATION
GEORGE C. MARSHALL SPACE FLIGHT CENTER
CONTRACT NO. NAS8-21086
HUNTSVILLE, ALABAMA

administered through:

OFFICE OF RESEARCH ADMINISTRATION

ANN ARBOR

November 1967

Engh
UMR
1378

ACKNOWLEDGMENTS

The author wishes to express his appreciation to Mr. George R. Carignan, Director of the Space Physics Research Laboratory, Department of Electrical Engineering, of The University of Michigan, for his advice and guidance throughout the period during which the work reported herein was performed. Further thanks go to Mr. Vernon H. Soden of the Space Physics Research Laboratory for his services in the design and technical construction of the system described in the present report. In addition, the author is indebted to Professor Louis F. Kazda, Department of Electrical Engineering, who served as chairman of his doctoral committee and continued to assist him in the performance of his research on the project reported.

This research was supported by the National Aeronautics and Space Administration, Contract No. NAS8-21086, and administered through the George C. Marshall Space Flight Center, Huntsville, Alabama.

TABLE OF CONTENTS

	Page
LIST OF FIGURES	v
ABSTRACT	vi
1. INTRODUCTION	1
2. A DESCRIPTION OF THE SPACE PHYSICS RESEARCH LABORATORY ULTRAHIGH VACUUM SYSTEM	1
3. THE MATHEMATICAL MODEL OF THE VACUUM SYSTEM	2
3.1 The Vacuum Chamber and Pump Piping Model	2
3.2 The Variable Leak Valve Model	6
3.3 The Ionization Gauge Controller Model	9
3.4 Model of the Driving Motor and Gear Train	11
4. OPTIMIZATION OF THE VACUUM SYSTEM BY USING THE MODERN CONTROL THEORY	13
4.1 Reformation of the Mathematical Model	13
4.2 The Optimization Criterion	15
4.3 The Practical Implementation	17
5. A SUB-OPTIMAL SYSTEM	17
6. REFERENCES	20

LIST OF FIGURES

Figure	Page
1. Plant of the ultrahigh vacuum system.	2
2. Schematic diagram of the vacuum system.	4
3. Electric circuit analog of the vacuum system.	4
4. Leak-valve sealing mechanism.	7
5. Driving mechanism.	7
6. Leak rate vs. turns.	8
7. The Granville-Phillips ionization gauge controller as a portion of the vacuum system.	9
8. Vacuum system characteristics.	10
9. Block diagram of the vacuum system.	11
10. The driving motor.	12
11. The coulomb friction force introduced in the vacuum system.	12
12. State space for the vacuum system.	16
13. Schematic diagram of the optimal vacuum system.	16
14. Maurer servo amplifier.	17
15. Chopper and voltage amplifier stage.	18
16. Differential amplifier and compensating circuit.	19
17. Block diagram of the sub-optimal system.	19

ABSTRACT

The problem of mathematically modeling the ultrahigh vacuum system and of determining methods for the optimizing of its performance is discussed in the report "On the Optimization of the Space Physics Research Laboratory Ultrahigh Vacuum System."

The approach used is the utilization of modern control theory methods to synthesize a control scheme which optimizes the system performance with respect to a predetermined cost function.

A sub-optimal controller for the system is then presented which overcomes the financial problems associated with the optimal system that beset a truly optimal system.

1. INTRODUCTION

In the Space Physics Research Laboratory at The University of Michigan, an attempt to optimize the performance of the existing vacuum system according to a prescribed criterion has been made. The techniques of modern control theory have been applied. Before its construction, the resulting controller has been investigated from the economical and practicable points of view. If the optimal system controller cannot be implemented practicably, then consideration should be given to the use of a classical controller. In addition, if the optimal system proves to be uneconomical, an investigation should also be made for the use of a sub-optimal controller. Finally, the report includes a practical design for the construction of a controller which improves the performance of the existing vacuum system.

2. A DESCRIPTION OF THE SPACE PHYSICS RESEARCH LABORATORY ULTRAHIGH VACUUM SYSTEM

The ultrahigh vacuum system, designed and assembled at the Space Physics Research Laboratory, consists of the following components, each serving a specific purpose:

- a. The vacuum chamber, whose pressure must be controlled;
- b. The vacuum pump, which removes gases from the chamber;
- c. The leak valve, the device which varies the amount of gas leaking to the pressure-controlled chamber; and
- d. The pressure gauge, the component that senses the pressure in the vacuum chamber and makes it available for measuring and recording.

In order to study the vacuum system from the control system point of view, it is necessary to analyze the components listed above. When the system is studied from the control system point of view, other parts of the vacuum system, e.g., the oven for baking and other accessory equipment for performing experiments, are considered to have little or no effect.

For the vacuum system under study, the pressure is being controlled in an open-loop fashion. There is no way to compensate for disturbances in the system resulting from the outgassing effect of the walls or from the absorbing effect. Normally the operator is faced with two problems. The first one is set-

ting the valve position in order to have a desired pressure, a tedious operation which requires much time, even by an experienced operator. An overshoot due to the time lag introduced by the vacuum chamber, which consequently increases the settling time of the system, usually results. The second problem arises when a disturbance occurs in the system and changes the output pressure. Unless the system is monitored by the operator, the actual pressure may be significantly different from the desired value. The operator mentally computes the amount he must open or close the valve to correct the undesirable situation which has developed in order to restore the pressure to the desired value. Manual performance of the small variations in the opening or closing of the valve is difficult because of mechanical problems associated with the existing leak valves (primarily, backlash and valve nonlinear gain over the operating range) and because of the physical limitations of the human operator.

3. THE MATHEMATICAL MODEL OF THE VACUUM SYSTEM

The main objective of developing the mathematical model of the vacuum system is to optimize the performance of the vacuum system according to a defined optimization criterion. To do so first requires a definition of the plant and then the development of the mathematical model. The plant or the fixed portions of the vacuum system refer to the ultrahigh vacuum system (UHVS) components defined above and to the driving system. The driving system consists of a motor and a possible gear train. An a-c driving system will be used in order to avoid the difficulties usually associated with a d-c driving system. These components may be integrated into a schematic block diagram indicating their relationship to the overall system (Figure 1).

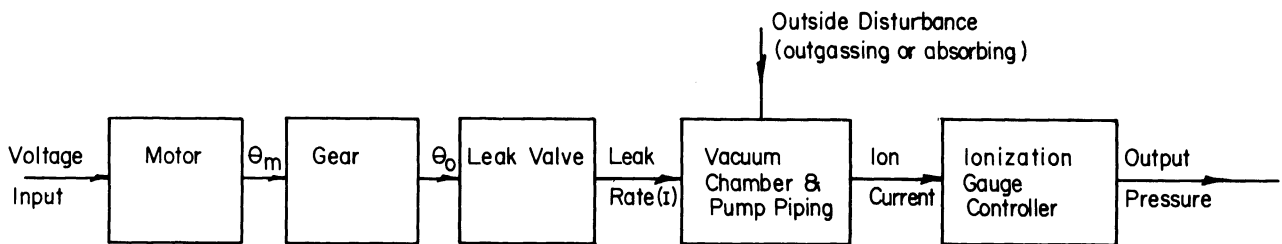


Figure 1. Plant of the ultrahigh vacuum system.

3.1 THE VACUUM CHAMBER AND PUMP PIPING MODEL

The vacuum chamber and pump piping model depends on the formulation of the electric circuit analog for a vacuum system. The idea of such an analog rests upon the fundamental similarity between the flow of gas in a vacuum system and that of the charge in an RC electric circuit (1,2). The scalar point function, electrical potential in electrical field theory, corresponds to the

scalar point function in gas flow pressure. Conservation of the scalar quantity charge corresponds to conservation of mass. The concept of electrical conductance of a conductor corresponds to the concept of a flow-conductance of a component of the vacuum system. The electrical capacity of a conductor corresponds to the volume of a vacuum system component.

By using these concepts, the electric circuit analog of the vacuum system, shown schematically in Figure 2, is given in Figure 3. The symbols introduced in Figure 3 are defined as follows:

I = Controlled variable leak rate source of the leak valve

I_d = Uncontrolled variable leak rate equivalent source of the absorption or outgassing of chamber walls

C_1 = Volume of the vacuum chamber

$G_1 = \frac{1}{R_1}$ = Conductance of the vacuum chamber

C_2 = Volume of pump piping

$G_2 = \frac{1}{R_2}$ = Conductance of pump piping

The system equation in the complex frequency domain for the model in Figure 3 yields

$$I(s) + I_d(s) = P(s) \left\{ sC_1 + \frac{1}{R_1 + \frac{R_2 \cdot \frac{1}{sC_2}}{R_2 + \frac{1}{sC_2}}} \right\}$$

By rearranging,

$$\frac{P(s)}{I(s) + I_d(s)} = \frac{R_1 + R_2 + C_2 R_1 R_2 s}{1 + [C_2 R_2 + C_1(R_1 + R_2)]s + C_1 C_2 R_1 R_2 s^2}$$

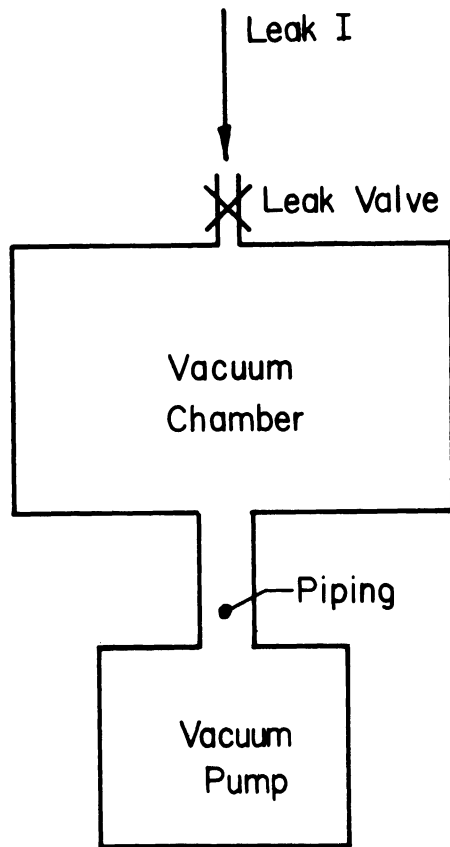


Figure 2. Schematic diagram of the vacuum system.

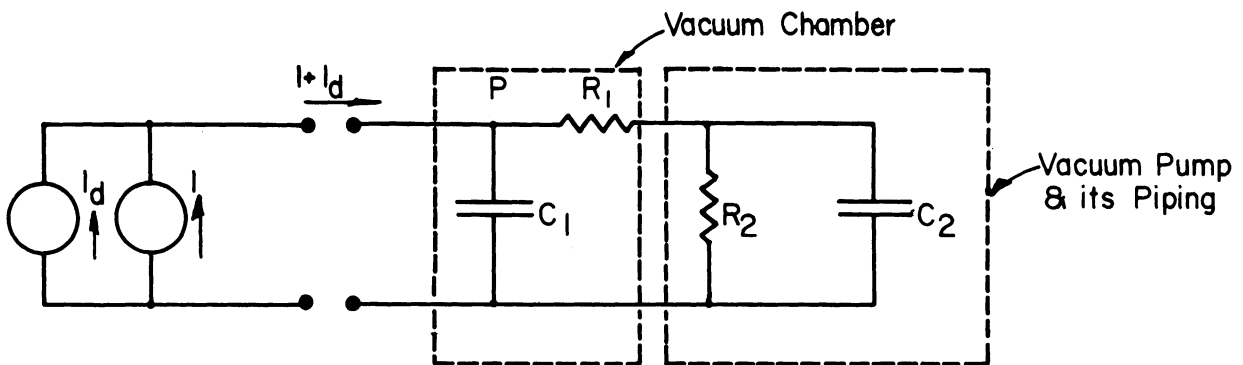


Figure 3. Electric circuit analog of the vacuum system.

It is evident from the dimensions of the vacuum system that $C_2 \ll C_1$ (chamber volume is much larger than pump piping volume). Therefore

$$\begin{aligned} \frac{P(s)}{I(s) + I_d(s)} &= \frac{1}{C_1} \left[\frac{s + \left(\frac{R_1 + R_2}{C_2 R_1 R_2} \right)}{s^2 + \frac{R_1 + R_2}{C_2 R_1 R_2} s + \frac{1}{C_1 C_2 R_1 R_2}} \right] \\ &= \frac{1}{C_1} \left[\frac{1}{s + \frac{1}{C_1(R_1 + R_2)} \left(1 + \frac{C_2 R_1 R_2}{R_1 + R_2} \right)^{-1}} \right] \end{aligned}$$

$$\frac{P(s)}{I(s) + I_d(s)} \approx (R_1 + R_2) \cdot \frac{1}{1 + C_1(R_1 + R_2)s}$$

This relation means that the vacuum chamber with the pump piping can be represented in the overall system by a gain $(R_1 + R_2)$ and a time constant $C_1(R_1 + R_2)$. This mathematical model is valid for all finite values of R_1 and R_2 (which are related to the speed of the pump), so long as the volume of the chamber is much larger than the volume of the pump piping.

For the vacuum system under consideration,

$$C_1 = 106l$$

$$C_2 = 2.36l$$

$$\begin{array}{l} R_1 = 0.2 \quad s/l \\ R_2 = 0.00667 \quad s/l \end{array} \left. \vphantom{\begin{array}{l} R_1 \\ R_2 \end{array}} \right] \text{For the normal operating speed of the pump}$$

$$\text{Time Constant} = 106 \times 0.20667$$

$$= 22 \text{ sec}$$

3.2 THE VARIABLE LEAK VALVE MODEL

The valve used in the variable leak system is made by the Varian Vacuum Division (3). It includes a movable piston with an optically-flat sapphire that meets a captured metal gasket. The movement of the sapphire is controlled through a threaded shaft-and-lever mechanism having a mechanical advantage of 13,000 to 1. Spring washers keep the drive mechanism constantly loaded in order to minimize backlash. The construction details are shown in Figures 4 and 5. Figure 6 shows the leak rate as a function of the knob turns. The valve component presents the major nonlinearity in the vacuum system. The mathematical model of this component consists only of a variable gain, since the dynamic behavior of the mechanical elements of the valve is neglected. Therefore, the valve as a component in the vacuum system has a zero time constant and a zero delay.

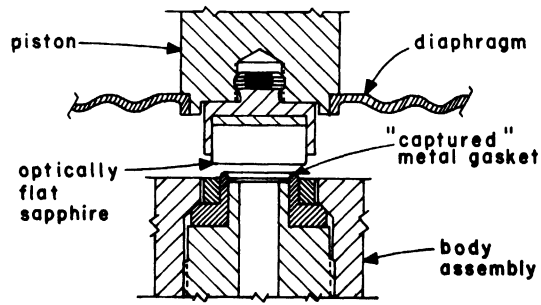


Figure 4. Leak-valve sealing mechanism.

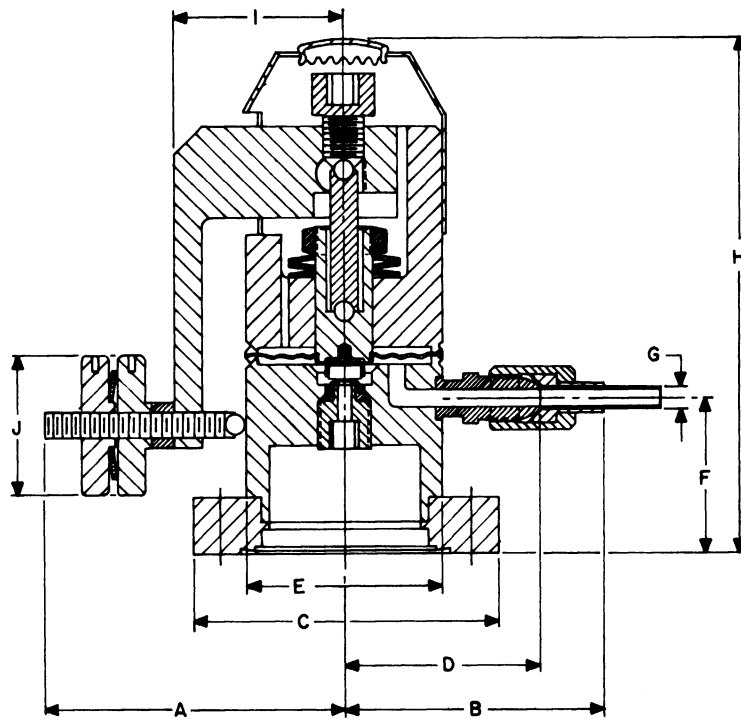


Figure 5. Driving mechanism.

	A	B	C	D	E	F	G	H	I	J
Inches	$2 \frac{21}{32}$	$2 \frac{3}{32}$	$2 \frac{3}{4}$	$1 \frac{3}{4}$	$1 \frac{3}{4}$	$1 \frac{5}{16}$	$\frac{1}{4}$	$4 \frac{1}{2}$	$1 \frac{17}{32}$	$1 \frac{1}{4}$
mm	67	53	70	44	44	33	6.4	114	39	32

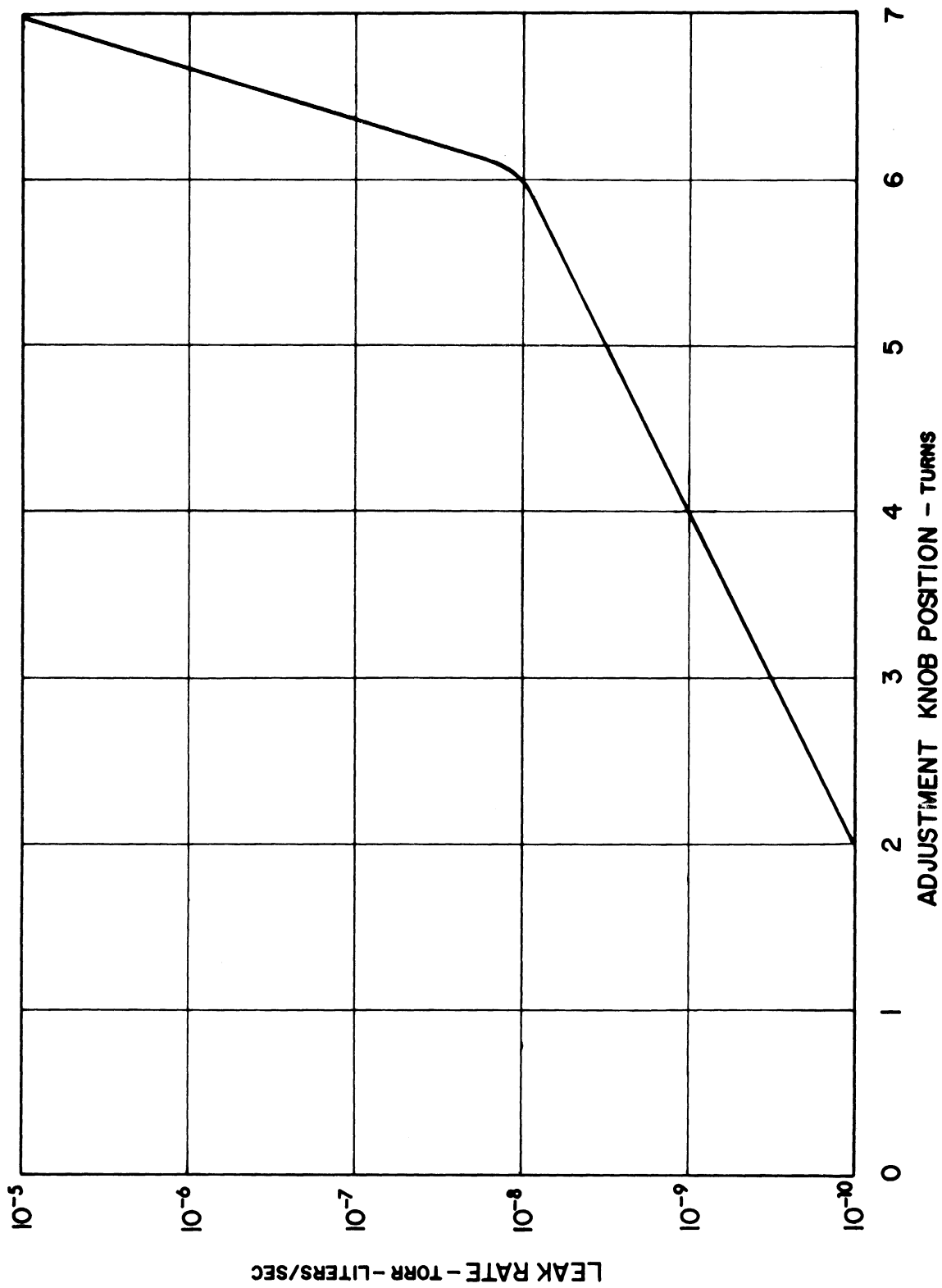


Figure 6. Leak rate vs. turns.

3.3 THE IONIZATION GAUGE CONTROLLER MODEL

Figure 7 represents a schematic diagram of the Granville-Phillips Company Controller used to sense and measure the pressure in the vacuum system. For more details, the reader is referred to the controller manual (4). By considering the chamber pressure as its input and the voltage reading as the output, such an instrument is linear over each operating range. Its time constant is less than 0.5 second.

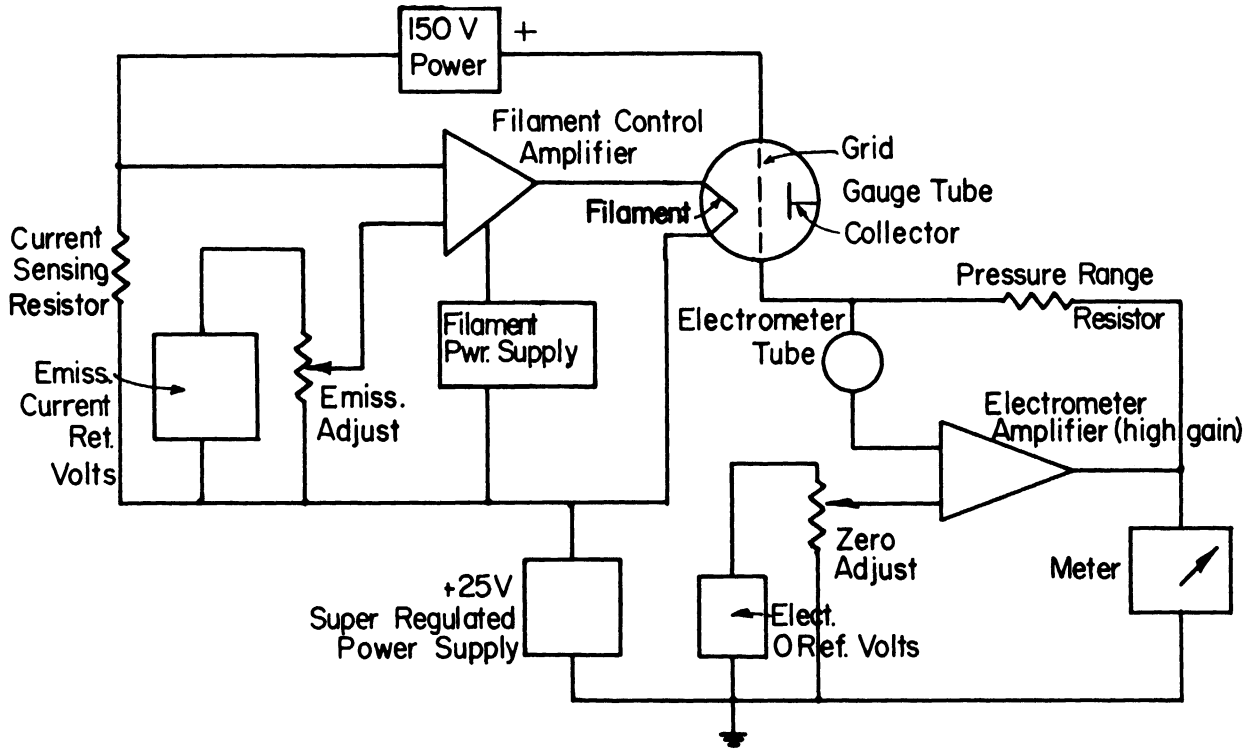


Figure 7. The Granville-Phillips ionization gauge controller as a portion of the vacuum system.

An experimental test has been made in order to determine the combined characteristics of the three components listed above, the valve, the chamber, and the ion gauge controller. The input, which is the knob rotation, is in degrees, and the output is the voltage read by a digital voltmeter connected across the output of the ion gauge controller. Three curves, obtained for three different ranges of the ion gauge controller, are illustrated in Figure 8. The curves represent steady-rate readings. The nonlinearity of the system is primarily due to the valve characteristics.

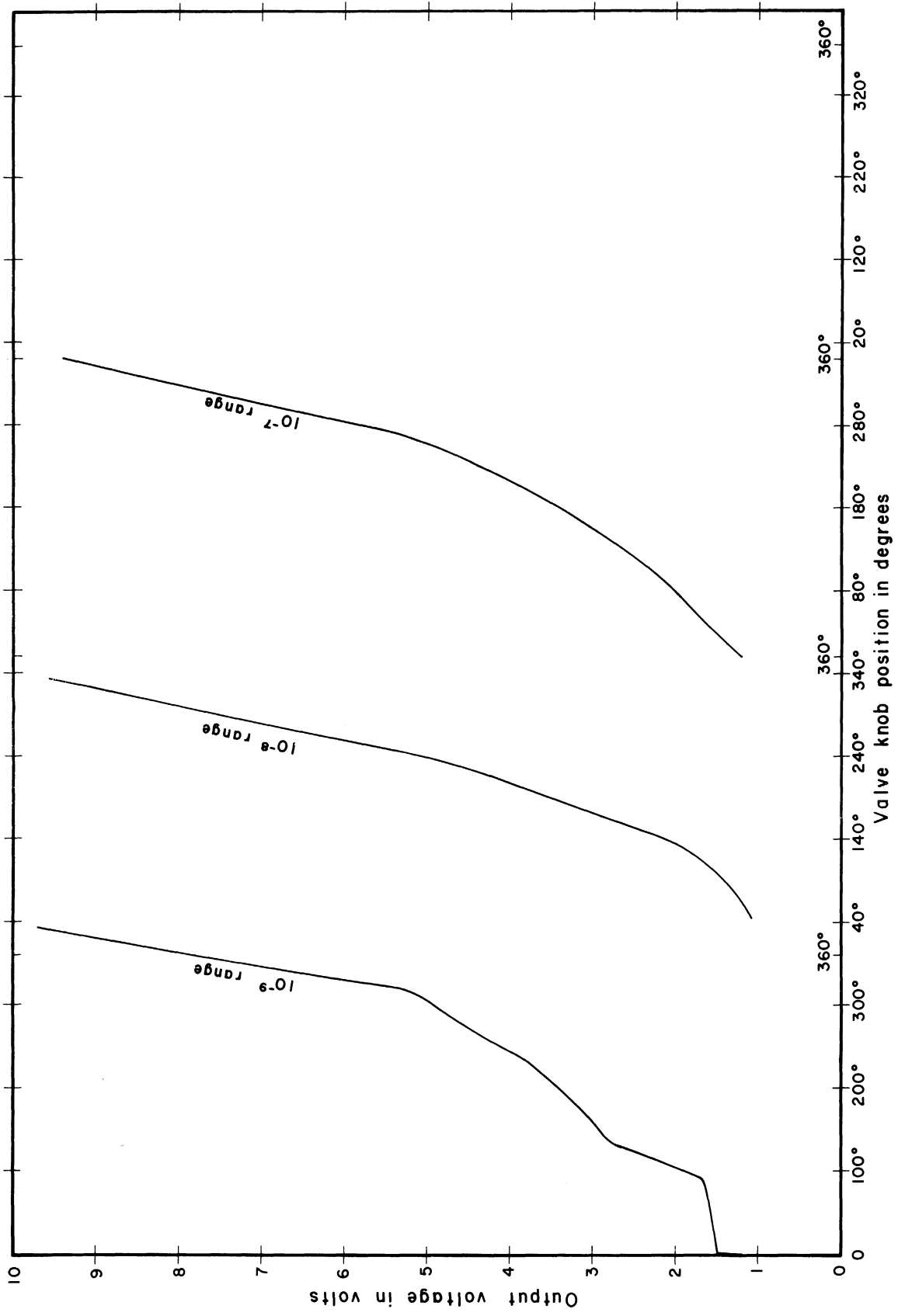


Figure 8. Vacuum system characteristics.

The equations representing the vacuum system in the time domain take now the following form:

$$P(t) + C_1(R_1 + R_2) \dot{P}(t) = (R_1 + R_2) [I(t) + I_d(t)]$$

and

$$I(t) = F[\theta_o(t)]$$

where F is a nonlinear function of the input $\theta_o(t)$, and $\dot{P}(t)$ is the time derivative of the chamber pressure. If τ_g is the time constant of the ionization gauge controller, the pressure $P(t)$ and the voltage reading $V(t)$ of the ion gauge controller can be related as follows:

$$\tau_g \dot{V}(t) + V(t) = K_g P(t)$$

Where $\dot{V}(t)$ is the time derivative of the voltage reading, K_g is the gain of the ionization gauge controller. Figure 9 is a block diagram of the vacuum system.

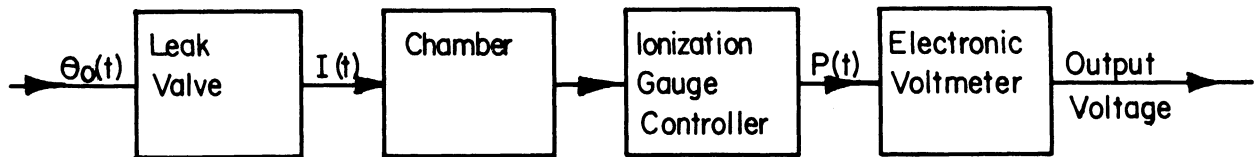


Figure 9. Block diagram of the vacuum system.

3.4 MODEL OF THE DRIVING MOTOR AND GEAR TRAIN

In small-power control systems, where the maximum output required from the motor ranges from a fraction of a watt up to a few hundred watts, 2-phase induction motors are used. The torque required to drive the leak valve has been measured and has been found to be approximately 4 oz-in. A FPE25-11, Navy type CDA-211052 Diehl a-c control-servo motor is suggested as the driver. The motor consists of a stator with two windings displaced 90 electrical degrees from each other and of a high resistance squirrel-cage rotor. Figure 10 represents a schematic diagram of the motor. A capacitor is used in order to establish the 90° phase shift. It can be shown (5,7) for such a motor that

$$\tau_m \frac{d^2 \theta_m}{dt^2} + \frac{d\theta_m}{dt} + C \sin(\dot{\theta}_o) = k_m v_i(t)$$

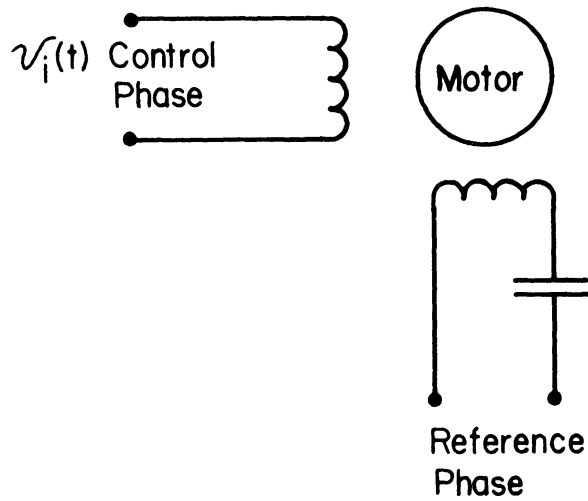


Figure 10. The driving motor.

Where τ_m is the time constant of the motor, $v_i(t)$ is the input voltage signal to the control winding of the motor, k_m is its gain, $\theta_m(t)$ is the position angle of the motor shaft, and $\theta_o(t)$ is the input position angle (angle of the valve knob shaft).

$$\text{Hence } \theta_o(t) = k_g \theta_m(t)$$

where $k_g = \text{gear ratio}$

It should be noted that the term $C \sin(\dot{\theta}_o)$ represents the coulomb friction force introduced in the system (Figure 11).

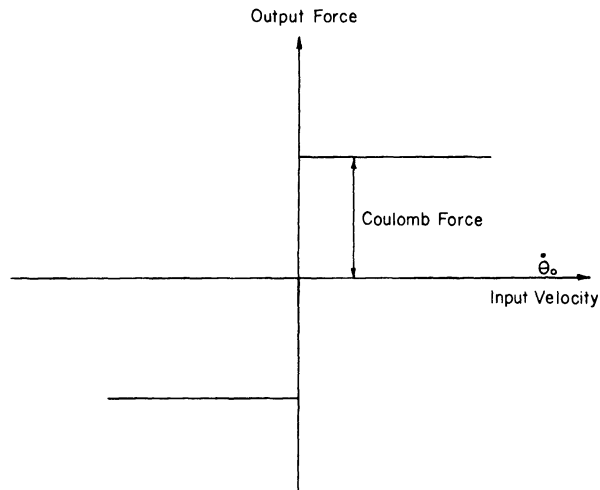


Figure 11. The coulomb friction force introduced in the vacuum system.

4. OPTIMIZATION OF THE VACUUM SYSTEM BY USING THE MODERN CONTROL THEORY

The mathematical model developed previously is used to formulate a method for optimally controlling the vacuum system in accordance with a prescribed performance criterion. The optimal problem is one of controlling the chamber pressure and of reducing the deviation from a prescribed reference value to zero, while at the same time minimizing the value of some predetermined performance of cost functional J . The development of the optimal control law proceeds essentially in four steps. The first step consists of a reformulation of the mathematical model in a form which is more suitable for the application of optimization techniques. In the second step, an optimization criterion is defined. In the third step, the particular optimization technique best suited for the optimization problem is chosen. Finally, in the fourth step, this optimization technique is utilized to construct the optimal control system.

4.1 REFORMATION OF THE MATHEMATICAL MODEL

It is convenient to begin by reformulating the equations representing the fixed portions of the vacuum system in the state variable formulation; i.e., in terms of a set of first order differential equations (8).

For the leak valve and the vacuum chamber, it has been shown that

$$P(t) + C_1(R_1 + R_2) \dot{P}(t) = (R_1 + R_2) [I(t) + I_d(t)]$$

$$I(t) = F [\theta_o(t)]$$

For the ionization gauge controller,

$$\tau_g \dot{V}(t) + V(t) = k_g P(t)$$

and for the driving motor and gear,

$$\tau_m \frac{d^2 \theta_m}{dt^2} + \frac{d\theta_m}{dt} + C \sin (\dot{\theta}_o) = k_m v_i$$

$$\theta_o(t) = k_g \theta_m(t).$$

Rearranging the equations which represent the fixed portion of the vacuum system results in

$$\dot{P}(t) = - \frac{1}{C_1(R_1 + R_2)} P(t) + \frac{1}{C_1} F [\theta_o(t)] + \frac{1}{C_1} I_d(t) \quad (1)$$

$$\dot{V}(t) = - \frac{1}{\tau_g} V(t) + k'_g P(t) \quad (2)$$

$$\dot{\theta}_o(t) = \theta_1(t) \quad (3)$$

$$\dot{\theta}_1(t) = - \frac{1}{\tau_m} \theta_1(t) + k_g k'_m v_i(t) - C \sin [\theta_1(t)] \quad (4)$$

Equations (1) through (4) represent an accurate state variable formulation of the vacuum system. For engineering purposes, however, the following approximations can be applied to the system without any appreciable error;

- a. The time constant of the ionization gauge controller can be neglected with respect to that of the vacuum chamber.
- b. The inertia of the load (leak valve shaft and accessories) can be neglected since the load is primarily due to coulomb friction.
- c. The characteristics of the valve can be assumed parabolic, i.e., $I(t) = k_v \theta_o^2(t)$, as observed from the experimental curves.

Equations (1) through (4) now take the following form:

$$\dot{P}(t) = - \frac{1}{C_1(R_1 + R_2)} P(t) + \frac{1}{C_1} k_v \theta_o^2(t) + \frac{1}{C_1} I_d(t)$$

$$V(t) = k'_g P(t)$$

$$\dot{\theta}_o(t) = \theta_1(t)$$

$$\dot{\theta}_1(t) = - \frac{1}{\tau_m} \theta_1(t) + k_g k'_m v_i(t) - C' \sin [\theta_1(t)]$$

Writing these equations in terms of the observable state variables, the following equations are obtained:

$$\dot{V}(t) = - \frac{1}{C_1(R_1 + R_2)} V(t) + \frac{k_v k'_g}{C_1} \theta_o^2(t) + \frac{k'_g}{C_1} I_d(t) \quad (5)$$

$$\dot{\theta}_o(t) = - C' \sin [\dot{\theta}_o(t)] + k_g k'_m v_i(t) \quad (6)$$

Equation (6) can be represented by the following two equations valid in the operating ranges of $\dot{\theta}_o(t)$.

$$\dot{\theta}_o(t) = - C' + k_g k'_m v_i(t) \quad \dot{\theta}_o(t) > 0 \quad (7)$$

$$\dot{\theta}_o(t) = C' + k_g k'_m v_i(t) \quad \dot{\theta}_o(t) < 0 \quad (8)$$

The primed quantities are evident from equations (1) through (4).

4.2 THE OPTIMIZATION CRITERION

For a given dynamic system, the optimization criterion may assume a variety of forms, depending on the requirement to be met. The choice of the optimization criterion is an important step in the design of the vacuum system since it determines to large degree the nature of the resulting optimal controller. The main objective in the optimization of the vacuum system at the Space Research Laboratory, The University of Michigan, is to obtain different levels of pressure in a minimum time, and to compensate for any resulting disturbances. Disturbances in the system result primarily from either absorption or outgassing, and are usually minimized by baking the system before operation. Therefore, the major concern is to bring the system from one level of pressure to another in minimum time. The optimal problem now is to choose a control $v_i^*(t)$ such that it satisfies the differential equations (5), (7), and (8), that it also satisfies the initial and final conditions, and that it concurrently minimizes the following functional form:

$$J = \int_{t_1}^{t_2} dt$$

where: t_1 = initial time

t_2 = final time

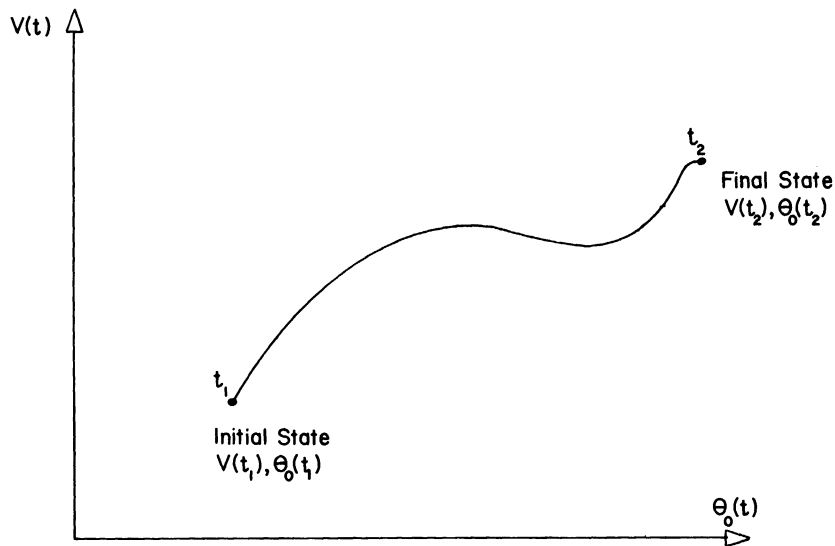


Figure 12. State space for the vacuum system.

It is apparent from the nonlinearity of equations (5) and (6) representing the system, that the solution for the optimal controller is a very difficult, if not impossible, task. The resulting optimal controller must sense the state variables of the system: the voltage read by the ionization gauge controller $V(t)$, and the output angle of the load $\theta_0(t)$. These state variables are then fed back through time-varying gains K_1 and K_2 . The gains are, in general, functions of the state variables $\theta_0(t)$ and $V(t)$, the initial conditions, the disturbance $I_d(t)$, and the time t . Consequently, the optimal control signal $v_1^*(t)$ is a nonlinear function of the state variables. In block diagram form, the optimal control system may be schematically represented as shown in Figure 13.

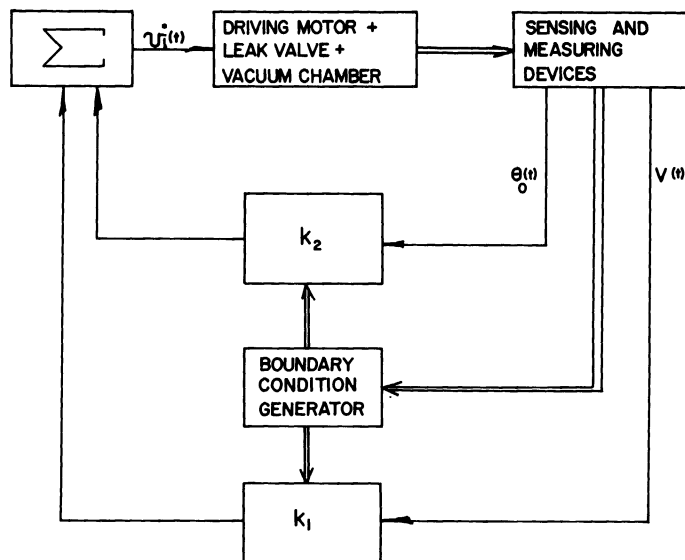


Figure 13. Schematic diagram of the optimal vacuum system.

4.3 THE PRACTICAL IMPLEMENTATION

It is apparent from the complexity of the optimal feedback control system that a computer is needed in order to synthesize such a scheme. Therefore, before one attempts to obtain optimal solutions numerically, one should first consider the possibility that a classical controller might do almost as well as the optimal one. Since the optimal controller is uneconomical for the purposes of the Space Physics Laboratory at The University of Michigan, an investigation has been made for the use of a sub-optimal controller.

5. A SUB-OPTIMAL SYSTEM

The problem of assembling a servo system in the classical way seems straightforward. A motor which is capable of driving the given load under the worst condition is chosen. The FPE25-11 Navy type CDA-211052 Diehl a-c control-servo motor is a suitable driver for the leak valves, through a 250:1 gear system. An amplifier is then selected with sufficient power output to drive the motor to its full torque rating. A Maurer power amplifier (available at the Space Physics Research Laboratory), is selected to supply the driving motor with the necessary power. This amplifier is capable of supplying up to 50w. It also has a gain control. The circuit diagram of this amplifier is shown in Figure 14. In order to produce adequate voltage output

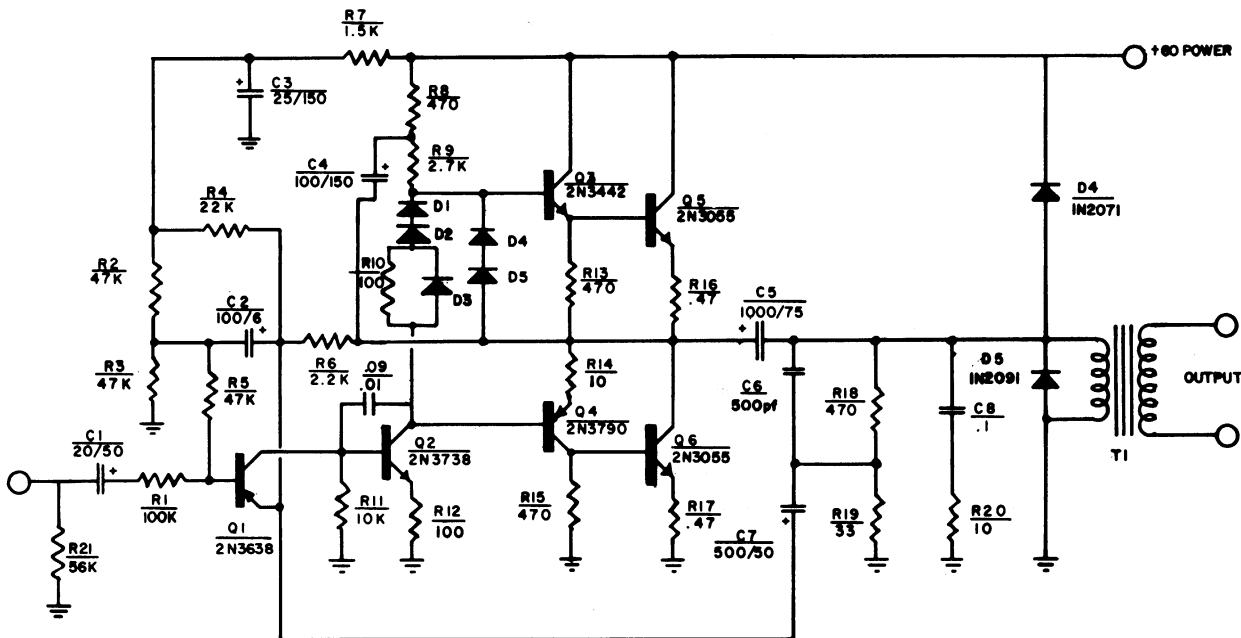
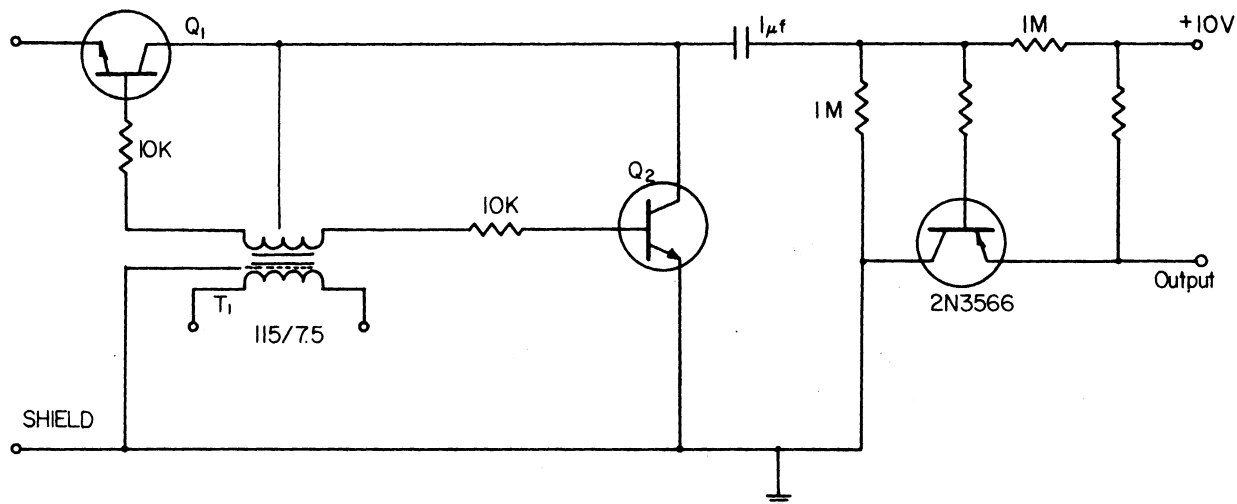


Figure 14. Maurer servo amplifier.

per degree of shaft rotation, a voltage amplifier stage is used to supply the necessary voltage amplification. A chopper is also needed to convert the d-c error signal to a proportional a-c one. The chopper and the voltage amplifier stage are illustrated in Figure 15. If this system is assembled (including a feedback loop from the ion gauge controller), it could be unstable. It could also swing back and forth about the final value, taking an inordinately long time to settle to rest. These types of responses are due to time lags in the system contributed mainly by the vacuum chamber together with time constants in the amplifier and associated electronics.



Q₁ = GE 2N2193
 Q₂ = GE 2N2193
 T₁ = OSBORNE 21549

Figure 15. Chopper and voltage amplifier stage.

Normally the feedback voltage from the output opposes or subtracts from that of the input, so that as the error increases, the restoring torque also rises. If the time lag between the system input and output becomes great enough, the feedback voltage reverses polarity and adds to the input. Such reversal causes the error to increase rather than to decrease. The overswing continues until the voltage and torque saturation level of the system is reached. In this case, the system will oscillate continuously. The required stability and the minimization of the dynamic errors in the system are provided by the use of electrical compensating networks, since, for mechanical reasons, the use of a tachometer generator is not desired. Such a compensating circuit is shown in Figure 16. Because of the extreme nonlinear behavior of the leak valve, the parameters of the compensating network are determined experimentally by trial and error. In order to produce the error signal from the reference and the actual signals and also to eliminate impedance level problems, a differential amplifier is then necessary in the system. The differential amplifier and compensating circuit are shown in Figure 16. It should be noted that the reference signal is produced by a highly accurate

10v power supply through an accurate 10-turn potentiometer. The actual signal is the output of the ion gauge controller.

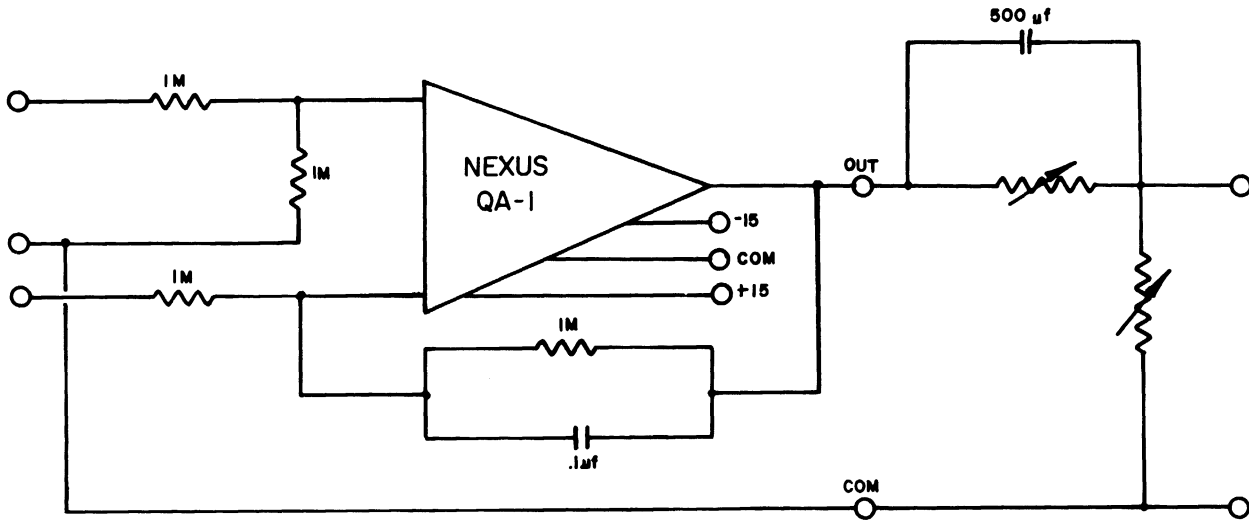


Figure 16. Differential amplifier and compensating circuit.

By experimental trial and error, the above method of assembling the servo system, a classical controller or a sub-optimal controller results. Such a sub-optimal controller can be implemented practicably and is economically feasible. Figure 17 is a block diagram of the suggested sub-optimal system

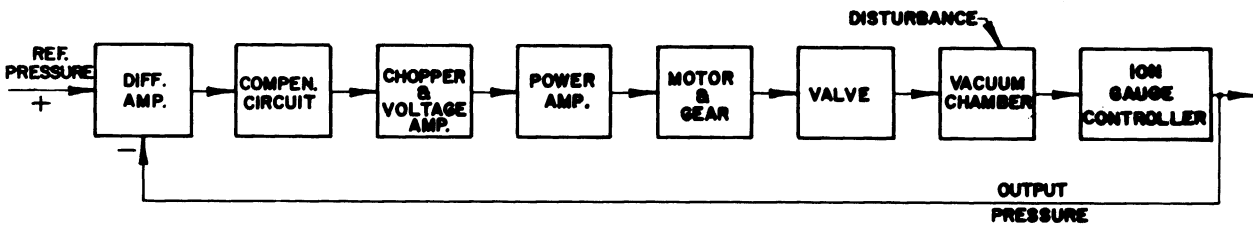


Figure 17. Block diagram of the sub-optimal system.

6. REFERENCES

1. Roberts, Richard W. and Vanderslice, Thomas A., Ultrahigh Vacuum and Its Applications, Prentice-Hall, Inc., Englewood Cliffs, New Jersey, 1963.
2. Barrington, Alfred E., High Vacuum Engineering, Prentice-Hall, Inc., Englewood Cliffs, New Jersey, 1963.
3. "Variable Leak Valve Data Sheet," Varian Associates, Vacuum Division, 611 Hansen Way, Palo Alto, California 94303.
4. "Operating Instructions for Series 236 Model 02 Ionization Gauge Controller," Granville-Phillips Company, 5675 E. Arapahoe Avenue, Boulder, Colorado 80302.
5. Fitzgerald, Arthur E. and Kingsley, Charles, Jr., Electric Machinery, McGraw-Hill Book Company, Inc., New York, p. 568.
6. Eltimsahy, Adel H., The Optimization of Domestic Heating Systems, Ph.D. Thesis, Department of Electrical Engineering, University of Michigan, April, 1967 (unpublished).
7. Thaler, George J. and Pastel, Marvin P., Analysis and Design of Nonlinear Feedback Control Systems, McGraw-Hill Book Company, New York, 1962, p.464.
8. Tou, Julius T., Modern Control Theory, McGraw-Hill Book Company, New York, 1964.

UNIVERSITY OF MICHIGAN



3 9015 02826 7485